EUROPEAN JOURNAL OF CANCER 48 (2012) 827–836

available at www.sciencedirect.com

ScienceDirect

journal homepage: www.ejconline.com

The functional significance of miR-1 and miR-133a in renal cell carcinoma

Kazumori Kawakami [a], *Hideki Enokida* [a,*], *Takeshi Chiyomaru* [a], *Shuichi Tatarano* [a], *Hirofumi Yoshino* [a], *Ichiro Kagara* [a], *Takenari Gotanda* [a], *Tokushi Tachiwada* [a], *Kenryu Nishiyama* [a], *Nijiro Nohata* [b], *Naohiko Seki* [b], *Masayuki Nakagawa* [a]

[a] *Department of Urology, Graduate School of Medical and Dental Sciences, Kagoshima University, Kagoshima, Japan*
[b] *Department of Functional Genomics, Graduate School of Medicine, Chiba University, Chiba, Japan*

ARTICLE INFO

Article history:
Available online 11 July 2011

Keywords:
TAGLN2
MicroRNA
MiR-1
MiR-133a
Renal cell cancer

ABSTRACT

Purpose: The aim of this study was to find a novel molecular network involved in renal cell carcinoma (RCC) development through investigating the functions of miR-1 and miR-133a and their target genes.

Methods: We checked the expression levels of miR-1 and miR-133a in RCC cell lines and specimens ($N = 40$) using real time RT-PCR. MiR-1 and miR-133a transfectants were subjected to a gain-of-function study to identify the functions of the miRNAs. To find the target genes of the miRNAs, we analysed the gene expression profile of their transfectants and performed a luciferase reporter assay. mRNA expression levels of the candidate target gene in the clinical specimens were examined, and loss-of-function studies were performed.

Results: The expression levels of miR-1 and miR-133a were significantly suppressed in RCC cell lines and specimens. Ectopic restoration of miR-1 and miR-133a showed significant inhibition of cell proliferation and invasion, and moreover, revealed induction of apoptosis and cell cycle arrest. The luciferase assay revealed transgelin-2 (TAGLN2), selected as a target gene for miR-1 and miR-133a on the basis of the gene expression profile, to be directly regulated by both miR-1 and miR-133a. The loss-of-function studies showed significant inhibitions of cell proliferation and invasion in the si-TAGLN2 transfectant. The expression level of TAGLN2 mRNA was significantly up-regulated in the RCC specimens; in addition, there was a statistically significant inverse correlation between TAGLN2 and miR-1 and miR-133a expression.

Conclusions: Our data indicate that up-regulation of the oncogenic TAGLN2 was due to down-regulation of tumour-suppressive miR-1 and miR-133a in human RCC.

1. Introduction

Renal cell cancer (RCC) is one of the major human malignancies and a leading cause of cancer mortality, and clear cell RCC represents the most common renal cancer histology.[1] Despite the trend of increased incidence of relatively small and kidney-confined disease, the rate of mortality has not changed significantly during the last two decades.[2,3] MiRNAs are small regulatory RNA molecules that modulate the expression of their target genes and play important roles in

* *Corresponding author*: Address: Department of Urology, Graduate School of Medical and Dental Sciences, Kagoshima University, 8-35-1 Sakuragaoka, Kagoshima 890-8520, Japan. Tel.: +81 99 275 5395; fax: +81 99 265 9727.
E-mail address: enokida@m.kufm.kagoshima-u.ac.jp (H. Enokida).
0959-8049/$ - see front matter
doi:10.1016/j.ejca.2011.06.030

a variety of physiological and pathological processes, such as cell proliferation and apoptosis.[4] The discovery of miRNAs adds another mechanism for gene regulation in human disease, including cancer.[5] Expression data and experimental evidence indicate that miRNAs frequently acquire a gain or a loss of function in cancer and that miRNAs play a crucial role in the development of cancer.[6,7] We previously reported that miR-1 and/or miR-133a, clustered at chromosome 18 and 20, have a tumour-suppressive function in human bladder cancer.[8–12] Moreover, other investigators have shown that miR-1 and miR-133a are down-regulated in bladder cancer.[13] Regarding other types of cancer, miR-1 has been reported to be down-regulated in gastric cancer,[14] rhabdomyosarcoma,[15,16] colon cancer,[17] lung cancer,[18] prostate cancer[19] and liver cancer,[20] while miR-133a has been reported to be down-regulated in head and neck cancer,[21] rhabdomyosarcoma,[15] oesophageal cancer,[22] colon cancer[17] and tongue cancer.[23] However, the expression and functions of miR-1 and miR-133a are never yet to be investigated in RCC. The aim of this study was to find a novel molecular network involved in RCC development by investigating the functional role of miR-1 and miR-133a through gain-of-function studies in RCC cell lines and to find the target genes of miR-1 and miR-133a.

2. Materials and methods

2.1. Patients

A total of 40 pairs of clear cell type tumour and adjacent normal tissue were collected from patients immediately they had undergone radical nephrectomies at Kagoshima University Hospital. The samples were processed and stored in RNAlater (QIAGEN, Valencia, CA, USA) at −20 °C until the RNA extraction. The patients' information is summarised in Table 1. These samples were staged according to the American Joint Committee on Cancer-Union Internationale Contre le Cancer (UICC) tumour-node-metastasis classification and histologically graded.[24] Our study was approved by the Bioethics Committee of Kagoshima University; written prior informed consent and approval were given by the patients.

Table 1 – Patients' characteristics.

	n	(%)
Total number	40	
Age (mean ± SD) 36–87 (64.1 ± 13.6)		
Gender		
Male	27	(67.5)
Female	13	(32.5)
Pathological tumour stage		
pT1a	20	(50.0)
pT1b	12	(30.0)
pT2	2	(5.0)
pT3a	3	(7.5)
pT3b	3	(7.5)
pT4	0	(0.0)
Grade		
G1	8	(20.0)
G2	30	(75.0)
G3	0	(0.0)
unknown	2	(5.0)
Infiltration		
α	28	(70.0)
β	12	(30.0)
γ	0	(0.0)
Venous invasion		
v (−)	30	(75.0)
v (+)	10	(25.0)

2.2. Cell culture and RNA extraction

We used two human RCC cell lines, 786-O and A498, obtained from the American Type Culture Collection (Manassas, VA, USA). The cell lines were incubated in RPMI 1640 medium supplemented with 10% fetal bovine serum and maintained in a humidified incubator (5% CO_2) at 37 °C. Total RNA was extracted, as previously described.[9]

2.3. Quantitative real time RT-PCR

Stem-loop RT-PCR (TaqMan MicroRNA Assays®; P/N: PM10617 for miR-1, and PM10413 for miR-133a; Applied Biosystems, Foster City, CA, USA) was used to quantitate miRNAs according to the previously published conditions.[8] TaqMan primers for TAGLN2 (P/N: Hs00761239_m1; Applied Biosystems) were used to check the mRNA expression. To normalise the data for quantification of the miRNAs and TAGLN2 mRNA, we used RNU48 (P/N: 001006; Applied Biosystems) and human GUSB (P/N: Hs99999908_m1; Applied Biosystems), respectively, and we used the delta–delta C_t method to calculate the fold change. The fold changes of the clinical samples were normalised with the average of the delta C_t value of the all normal adjacent tissues. We used FirstChoice® Total RNA from normal human kidney (AM7976; Applied Biosystems) as a control of normal RNA for the RCC cell lines.

2.4. Transfection of mature miRNA and siRNA

Mature miRNA and siRNA were transfected, as previously reported.[8] Pre-miR™ precursors (Applied Biosystems), negative-control miRNA (Applied Biosystems), si-TAGLN2 (Cat#; HSS144746, Invitrogen) and negative control siRNA (D-001810-10; Thermo Fisher Scientific, Waltham, MA, USA) were used. We evaluated the transfection efficacy of the miRNAs in the RCC cell lines based on the down-regulation of protein tyrosine kinase 9 (PTK9) mRNA after miR-1 transfection as indicated manufacturer's protocol.

2.5. Cell proliferation assay and invasion assay

Cell proliferation assay (XTT assay) and invasion assay were performed according to the protocol designed in the previous report.[9] The results are shown as the percentage of the absorbance and migrated cells relative to the control. All experiments were performed in triplicate.

2.6. Flow cytometry

The 786-O and A498 cells transiently transfected with miR-control, miR-1, or miR-133a were harvested 72 h after transfection by trypsinisation. The apoptosis analysis was

done as previously described.[12] Cells for the cell cycle analysis were stained with PI using the CycleTEST™ PLUS DNA Reagent Kit (BD Biosciences, Bedfold, MA, USA) following the protocol and analysed by FACScan (BD Biosciences). The percentage of the cells in the G0/G1, S and G2/M phase were counted and compared. Experiments were done in triplicate.

2.7. *Target gene search for miR-1 and miR-133a*

Oligo-microarray Human 44,000 (Agilent) was used for expression profiling in miR-1- and miR-133a-transfected A498 cells in comparison with the miR-negative control transfectant, as previously described.[12] The microarray data were approved by the Gene Expression Omnibus (Accession Number: GSE19717).

2.8. *Western blots and luciferase assay*

Western blotting using TAGLN2 and GAPDH was performed in accordance with the previously reported protocol.[12] The protocol for plasmid construction and dual-luciferase reporter assay used in the previous study[12] was strictly followed in this study.

2.9. *Statistical analysis*

The relationship between two variables and the numerical values obtained by real-time RT-PCR was analysed using the Mann–Whitney *U*-test. The relationship among three variables and the numerical values was analysed using the Bonferroni-adjusted Mann–Whitney *U*-test. Spearman's rank test was used to evaluate the relationships among the relative expression levels of miR-1, miR-133a and mRNA levels of TAGLN2. All statistical analyses were performed using Expert StatView® analysis software (version 4; SAS Institute Inc., Cary, NC, USA).

3. Results

3.1. *Detection of the expression levels of miR-1 and miR-133a in RCC specimens and cell lines by quantitative stem-loop RT-PCR*

The expression levels of miR-1 and miR-133a were significantly lower in clinical RCC specimens than in adjacent normal tissues (each, $p < 0.0001$; Fig. 1A and B). Furthermore, there was a significant positive correlation between the

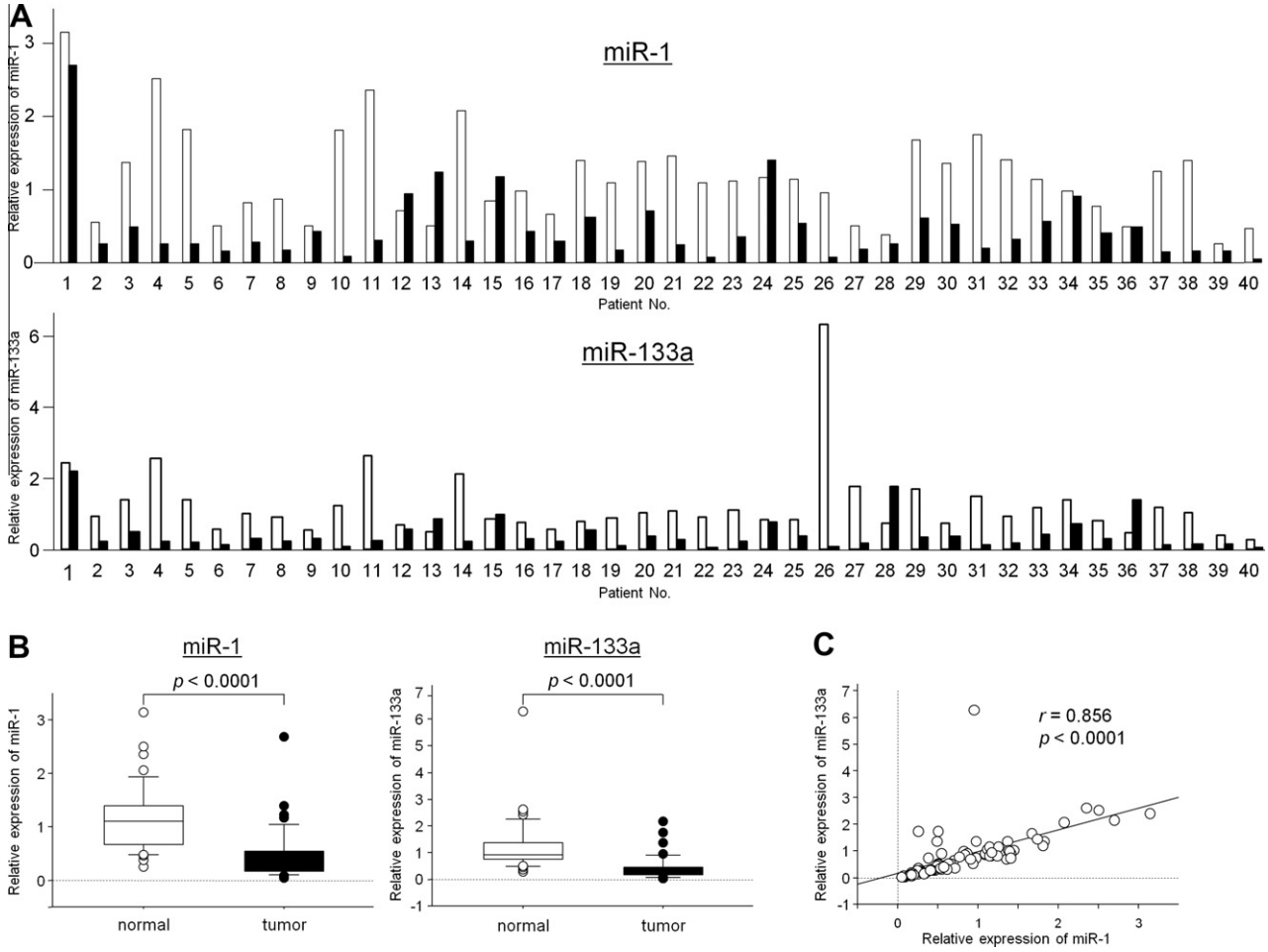

Fig. 1 – Expression levels of miR-1 and miR-133a in RCC specimens. (A) Normalised relative expression levels of miR-1 (upper) and miR-133a (lower) are shown in the bar chart. White and black bars indicate expression levels in normal and tumour tissues, respectively. (B) Relative expression levels of miR-1 (left) and miR-133a (right) are shown in a box plot. (C) Correlation between the relative expression levels of miR-1 (*x*-axis) and miR-133a (*y*-axis). Levels are plotted as a scatterplot.

expression levels of miR-1 and miR-133a ($r = 0.856$, $p < 0.0001$; Fig. 1C). MiR-1 and miR-133a were also significantly down-regulated in RCC cell lines, 786-O and A498, in comparison with normal kidney RNA (each, $p < 0.0001$; Fig. 2A). There was no significant relationship between the clinicopathological parameters (i.e. tumour stage, grade, infiltration or venous invasion) and the expression levels of miR-1 and miR-133a (data not shown).

3.2. *Effect of miR-1 and miR-133a restoration on cell proliferation and invasion in RCC cells*

To investigate the molecular functions of miR-1 and miR-133a, we performed a gain-of-function study using transient transfection with mature miR-1 and miR-133a. The XTT assay demonstrated that cell proliferation was significantly inhibited in miR-1 and miR-133a transfectants in comparison with the control in RCC cell lines (% of cell viability relative to control; 786-O, 18.3 ± 1.6 and 64.9 ± 4.1, respectively, each, $p < 0.0001$; A498, 28.6 ± 2.3 and 59.4 ± 4.5, respectively, each, $p < 0.0001$; Fig. 2B). The matrigel invasion assay demonstrated that invading cell numbers significantly decreased in both miR-1- and miR-133a-transfected RCC cell lines in comparison with the controls (% of cell invasion relative to control; 786-O, 13.9 ± 6.8 and 55.9 ± 6.4, $p < 0.0001$ and $p = 0.0004$, respectively; A498, 14.7 ± 3.9 and 28.2 ± 4.9, respectively, each, $p < 0.0001$; Fig. 2C).

3.3. *Effect of miR-1 and miR-133a restoration on apoptosis and cell cycle*

Because miR-1 and miR-133a restoration significantly inhibited cell proliferation in RCC cell lines, we hypothesised that their restoration induces apoptosis and/or cell cycle arrest and performed flow cytometry. As shown in the representative quadrant images in Fig. 3A (left), the apoptotic and early apoptotic fraction (upper right and lower right in the quadrant images, respectively) were greater in miR-1 and miR-133a transfectants than in the control. The relative apoptotic cell fraction (apoptotic plus early apoptotic cells) was significantly larger in miR-1 and miR-133a transfectants than in the control, except the miR-133a transfectant in the A498 cell lines (Fig. 3A, right). As for the cell cycle distribution, number of cells in the G2/M phase were significantly smaller in miR-1 transfectant but larger in miR-133a transfectant in comparison with the control (Fig. 3B). These results suggest that miR-1 restoration induces G0/G1 arrest particularly in A498 cell lines, whereas miR-133a restoration induces G2/M arrest in both cell lines.

3.4. *Identification of genes down-regulated by miR-1 and miR-133a restoration*

To find the target gene of miR-1 and miR-133a in RCC, we performed an oligo-microarray consisting of 44,000 genes using

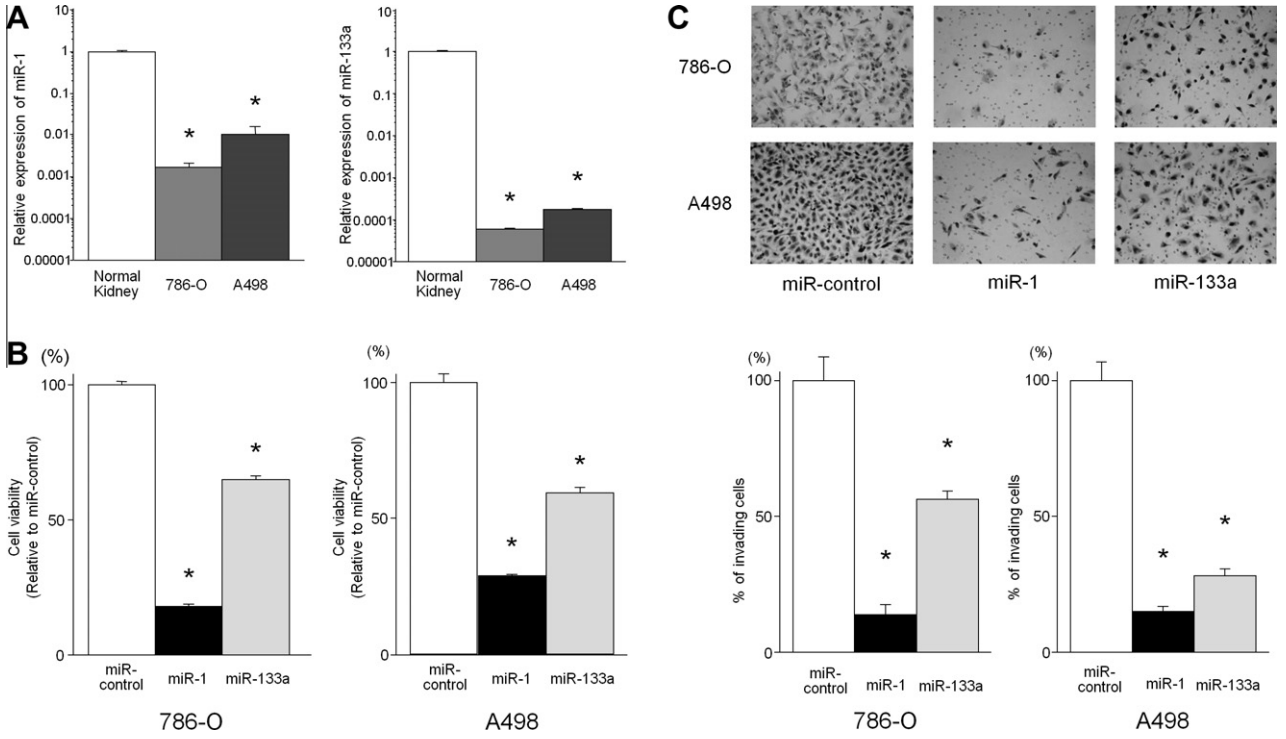

Fig. 2 – Tumour-suppressive function of miR-1 and miR-133a. (A) Expression levels of miR-1 (left) and miR-133a (right) were significantly down-regulated in RCC cell lines (786-O and A498) in comparison with normal kidney. *$p < 0.0001$. (B) Ectopic restoration of miR-1 or miR-133a significantly inhibited cell proliferation in 786-O (left) and A498 (right) cell lines in the XTT assay. *$p < 0.0001$. (C) Representative photos of invading cells in miR-control, miR-1-, or miR-133a-transfected cells in the matrigel membrane (upper). The bar graph expressed below the images of invasion assay indicated the relative value of the average invading cells in the miR-control, miR-1, or miR-133a transfectant (lower). *$p < 0.001$.

miR-1- and miR-133a- transfected A498 cell lines in comparison with the miR-control transfectant. The top 20 down-regulated genes in miR-1 and miR-133a transfectants are listed in Tables 2 and 3, respectively. We focused on transgelin-2 (TAGLN2) as a candidate target gene for both miR-1 and miR-133a because it was the only gene listed in both Tables. Moreover, we referred to a commercial web database (TargetScan) and found that TAGLN2 has a putative target site for both miR-1 and miR-133a in its 3′UTR region.

3.5. *TAGLN2 as a direct target for both miR-1 and miR-133a in RCC*

We performed real time RT-PCR and Western blotting to check that the mRNA and protein levels of TAGLN2 were down-regulated by restoring miR-1 and miR-133a. The mRNA and protein expression levels of TAGLN2 were markedly down-regulated in the miR-1 and miR-133a transfectants in comparison with the controls (Fig. 4A). Subsequently, we performed a luciferase reporter assay to determine whether TAGLN2 mRNA has actual target sites for miR-1 and miR-133a. We used a vector encoding full-length 3′UTR of TAGLN2 mRNA and found that the luminescence intensity was significantly reduced in the miR-1 and miR-133a transfectants (Fig. 4B). These results indicate that TAGLN2 is a common target gene for both miR-1 and miR-133a.

3.6. *Effect of TAGLN2 knockdown on cell proliferation and invasion in RCC cell lines*

To examine the functional role of TAGLN2, we performed loss-of-function studies using si-TAGLN2-transfected 786-O and A498 cell lines. The mRNA expression of TAGLN2 was innately higher in 786-O and A498 cell lines than in the control normal kidney (Fig. 5A). The effect of TAGLN2 knockdown was confirmed by conducting real time RT-PCR on both cell lines

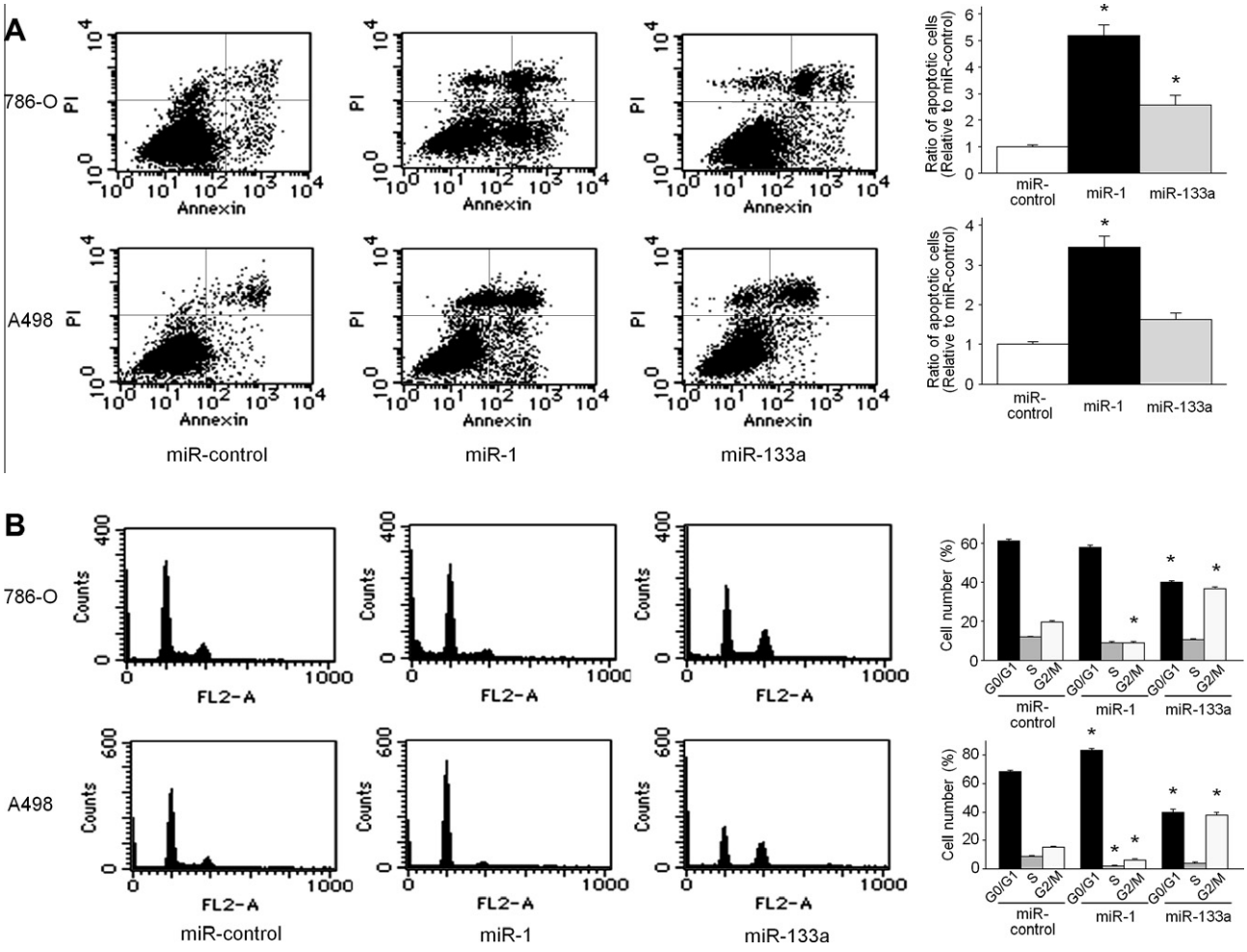

Fig. 3 – Effect of miR-1 and miR-133a restoration on apoptosis and cell cycle. (A) Representative quadrant figures of miR-control, miR-1, or miR-133a transfectants in 786-O (upper) and A498 (lower) cells. The bar chart shown on the right of each quadrant indicates the ratio of apoptotic cell fractions (early apoptotic plus apoptotic cells) in miR-1 or miR-133a transfectants in comparison with miR-control transfectant. Data for the apoptotic cell fractions are expressed as the relative value of the average expression of the miR-control transfectant. *$p < 0.05$. (B) Typical results of cell cycle analysis of miR-control, miR-1, or miR-133a transfectants. The bar chart shown on the right of each figure represents the percentage of the cells in the G0/G1, S, or G2/M phase.*$p < 0.001$.

Table 2 – Down-regulated genes in miR-1 transfectants.

Entrez gene ID	Symbol	Fold change (Log2 ratio)	Gene name	Putative binding sites
114902	C1QTNF5	−6.87	C1q and tumour necrosis factor related protein 5	(−)
81569	ACTL8	−5.08	Actin-like 8	(−)
8407	TAGLN2	−4.24	Transgelin 2	(+)
23446	SLC44A1	−4.21	Solute carrier family 44, member 1	(+)
113612	CYP2U1	−3.18	Cytochrome P450, family 2, subfamily U, polypeptide 1	(+)
9119	KRT75	−3.17	Keratin 75	(−)
2539	G6PD	−3.02	Glucose-6-phosphate dehydrogenase	(+)
5756	TWF1	−3.00	Twinfilin, actin-binding protein, homologue 1 (Drosophila)	(+)
79794	C12orf49	−2.84	Chromosome 12 open reading frame 49	(+)
1174	AP1S1	−2.80	Adaptor-related protein complex 1, sigma 1 subunit	(−)
84912	SLC35B4	−2.80	Solute carrier family 35, member B4	(+)
359845	FAM101B	−2.77	Family with sequence similarity 101, member B	(+)
2307	FOXS1	−2.75	Forkhead box S1	(−)
4050	LTB	−2.74	Lymphotoxin beta (TNF superfamily, member 3)	(−)
5757	PTMA	−2.61	Prothymosin, alpha	(+)
27230	SERP1	−2.61	Stress-associated endoplasmic reticulum protein 1	(+)
57530	CGN	−2.58	Cingulin	(−)
84650	EBPL	−2.50	Emopamil binding protein-like	(+)
6347	CCL2	−2.49	Chemokine (C-C motif) ligand 2	(+)
7117	TMSL3	−2.48	Thymosin-like 3	(+)

Table 3 – Down-regulated genes in miR-133a transfectants.

Entrez gene ID	Symbol	Fold change (Log2 ratio)	Gene name	Putative binding sites
8407	TAGLN2	−2.71	Transgelin 2	(+)
10952	SEC61B	−2.66	Sec61 beta subunit	(+)
2512	FTL	−2.47	Ferritin, light polypeptide	(+)
29956	LASS2	−2.46	LAG1 homologue, ceramide synthase 2	(+)
27166	PRELID1	−2.44	PRELI domain containing 1	(−)
10186	LHFP	−2.44	Lipoma HMGIC fusion partner	(+)
58472	SQRDL	−2.42	Sulphide quinone reductase-like (yeast)	(+)
10944	C11orf58	−2.39	Chromosome 11 open reading frame 58	(+)
7837	PXDN	−2.38	Peroxidasin homologue (Drosophila)	(+)
2744	GLS	−2.36	Glutaminase	(+)
81558	FAM117A	−2.36	Family with sequence similarity 117, member A	(+)
10746	MAP3K2	−2.32	Mitogen-activated protein kinase kinase kinase 2	(+)
200081	TXLNA	−2.31	Taxilin alpha	(+)
2512	FTL	−2.30	Ferritin, light polypeptide	(+)
1515	CTSL2	−2.29	Cathepsin L2	(+)
10092	ARPC5	−2.29	Actin related protein 2/3 complex, subunit 5, 16kDa	(+)
4833	NME4	−2.24	Non-metastatic cells 4, protein expressed in	(+)
1070	CETN3	−2.17	Centrin, EF-hand protein, 3 (CDC31 homologue, yeast)	(+)
55179	FAIM	−2.17	Fas apoptotic inhibitory molecule	(+)
79183	TTPAL	−2.10	Tocopherol (alpha) transfer protein-like	(+)

(Fig. 5B). The XTT assay revealed significant inhibition of cell proliferation in the si-TAGLN2 transfectants in comparison with the si-control transfectants (% of cell viability; 786-O, 21.5 ± 1.2 and 100.0 ± 3.5, respectively, $p < 0.0001$; A498, 36.5 ± 1.6 and 100.0 ± 3.4, respectively, $p < 0.0001$; Fig. 5C). The matrigel invasion assay demonstrated that the percentage of invading cells was significantly decreased in the si-TAGLN2 transfectants compared with the si-control (% of cell invasion; 786-O, 44.2 ± 7.5 and 100.0 ± 21.6, respectively, $p < 0.05$; A498, 22.5 ± 4.2, and 100.0 ± 9.9, respectively, $p < 0.05$; Fig. 5D). These results suggest that TAGLN2 has an oncogenic potential in the RCC cell lines.

3.7. *TAGLN2 mRNA expression in RCC specimens and its relationship with miR-1 and miR-133a expression*

The mRNA expression levels of TAGLN2 were significantly higher in the RCC specimens than in the adjacent normal tissues ($p < 0.0001$, Fig. 6A and B). Interestingly, there was a significant inverse correlation between the TAGLN2 mRNA expression and miR-1 and miR-133a expression ($r = -0.414$, $p = 0.0002$; and $r = -0.485$, $p < 0.0001$, respectively). No significant relationship was found between the clinicopathological parameters and the mRNA expression levels of TAGLN2 (data not shown).

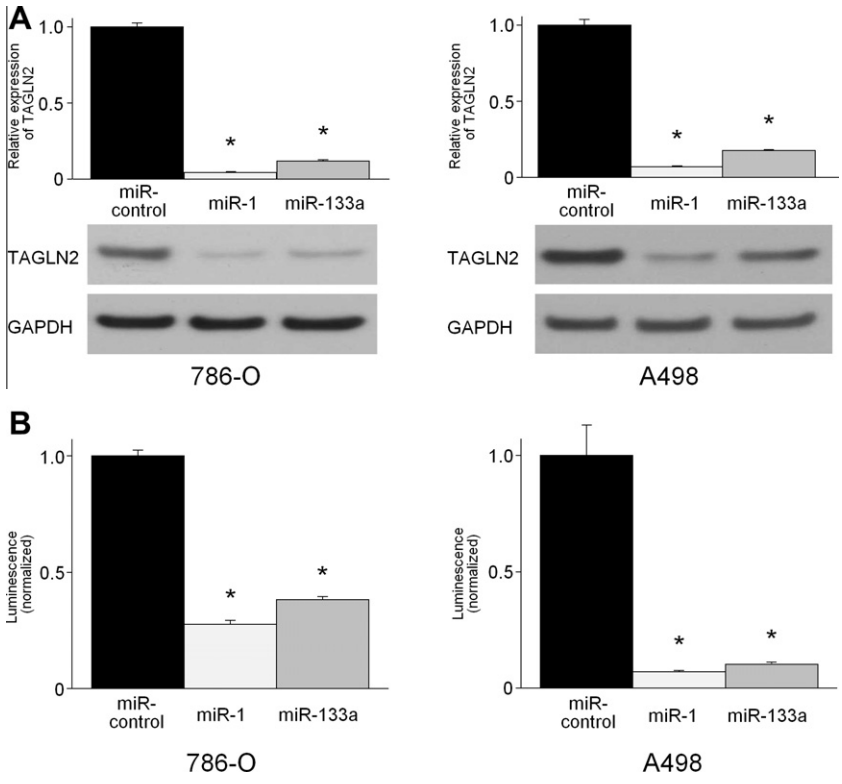

Fig. 4 – TAGLN2 as a target gene for both miR-1 and miR-133a. (A) mRNA expression levels of TAGLN2 were significantly down-regulated in both miR-1 and miR-133a transfectants in 786-O and A498 cells (upper left and upper right, respectively). *$p < 0.0001$. Down-regulation of TAGLN2 was also validated in protein levels by western blotting (lower photos). (B) Luciferase reporter assay using the vector encoding full-length 3′-UTR of TAGLN2 mRNA. *Renilla* luciferase values are normalised to the firefly luciferase values. Relative values of luminescence in miR-1 or miR-133a transfectants are shown. *$p < 0.001$.

4. Discussion

In this study, we found for the first time that both miR-1 and miR-133a function as tumour suppressors in RCC. There have been no reports concerning the down-regulation of miR-1 and miR-133a except for one report in which miR-1 was listed in the table as a down-regulated miRNA in RCC samples.[25] MiRNA expression profiles often differ due to the array platform used for the screening test. Previous studies have reported that miR-1 and miR-133a have tumour suppressive function, and these two miRNAs are clustered on the same chromosomal loci in several human malignancies.[12,13,15,17,19,22] In the majority of these reports, the investigators employed TaqMan low density array (LDA) Human microRNA Panel v2.0 (GPL 4133, Applied Biosystems), which we also used for the miRNA expression profile of bladder cancer.[12] In this study, we focused on miR-1 and miR-133a on the basis of previous miRNA profiles of other malignancies, but not on the basis of profiles of RCC. To our knowledge, there have been no submissions of the microRNA expression profile by using this platform for RCC. Consistent with previous reports, miR-1 and miR-133a were simultaneously down-regulated in the RCC cell lines and in a majority of the clinical samples. Furthermore, like the result in rhabdomyosarcoma,[15] there was a strong positive correlation between the miR-1 and miR-133a expression levels in the clinical specimens. Interestingly, miR-1 and miR-133 are clustered together on human chromosome 18 (18q11.2; miR-1-2 and miR-133a-1), where they are separated by 3.2 kb, and on human chromosome 20 (20q13.33; miR-1-1 and miR-133a-2), where they are separated by 10.5 kb. The fact that these miRNAs are close to each other might be the reason synchronous expression of these microRNAs was found in the majority of the cases. However, no synchronous expression of these microRNAs was observed in some of the clinical samples, and this raises a question as to where the each mature miRNA originates from (chromosome 18 or 20). Further studies are necessary to clarify this question.

The functions of miR-1 and miR-133a have been reported for several types of cancer, including bladder cancer,[8–12] rhabdomyosarcoma,[15,16] lung cancer,[18] liver cancer,[20] oesophageal cancer[22] and tongue cancer.[23] The consensus of these studies is that miR-1 and miR-133a have tumour-suppressive functions. In this study, the gain-of-function study also showed that miR-1 and miR-133a functioned as tumour suppressors in RCC cell lines by inhibiting cell proliferation and invasion and by promoting apoptosis and cell cycle arrest. Apoptosis and/or cell cycle analyses were performed using several cancer cell lines transfected with miR-1 and/or miR-133a, and the previous results were as follows; miR-1 and miR-133a: proapoptotic in bladder cancer,[11,12] miR-1: proapoptotic and arresting cell cycle in rhabdomyosarcoma,[15,16] miR-1: proa-

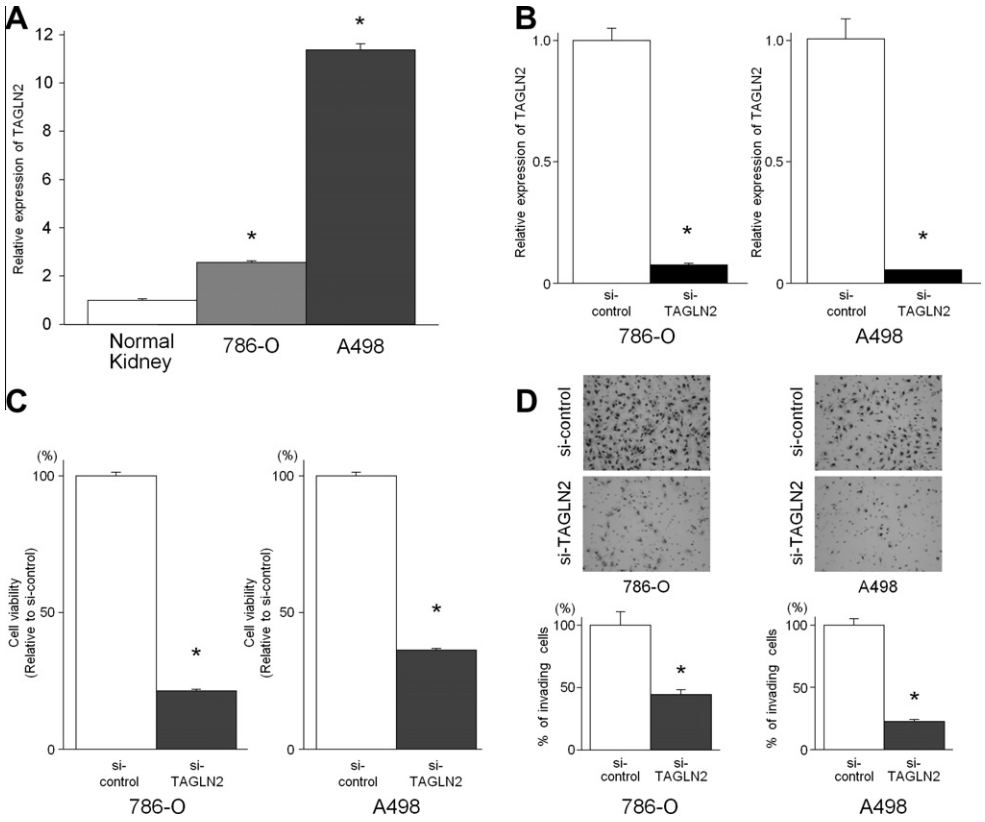

Fig. 5 – Effect of TAGLN2 knock down. (A) mRNA expression of TAGLN2 in RCC cell lines was greater than those of normal kidney. *$p < 0.001$. (B) The siRNA for TAGLN2 suppressed its mRNA expression. *$p < 0.05$. (C) Cell proliferation was significantly inhibited in si-TAGLN2 transfectant in comparison with the si-control in the XTT assay. *$p < 0.0001$. (D) Representative photos of invading cells in the si-control, or si-TAGLN2-transfected cells in the matrigel membrane (upper). The bar graph expressed below the images indicated the relative value of the average invading cells in the si-control or si-TAGLN2 transfectant (lower). *$p < 0.001$.

poptotic in lung cancer,[18] miR-1: proapoptotic and arresting cell cycle in liver cancer[20] and miR-1: proapoptotic in tongue cancer.[23] Consistent with these previous reports, the miR-1 and miR-133a restoration conducted for this report induced apoptosis in those transfected RCC cell lines. With regard to the cell cycle, miR-1 restoration caused G1 arrest in A498 cells, whereas miR-133a restoration induced G2 arrest in both cell lines. To our knowledge, this is the first report showing miR-133a is related to G2 arrest in cancer cell lines.

As a target gene for miR-1 and miR-133a, we identified TAGLN2, which contains a conserved actin-binding domain, indicating that TAGLN2 may be involved in cytoskeletal organisation[26]; however, the precise functions of TAGLN2 have yet to be explored. Our previous study revealed that other genes involved in cytoskeletal organisation, such as FSCN1 and LASP1, which contain actin-binding domain and were targeted by miR-1 or miR-133a, had oncogenic functions in bladder cancer.[9,10] These results suggest that several genes annotated on the cytoskeletal organisation with the actin-binding domain may have critical oncogenic functions in cancer development. We performed apoptosis and cell cycle analyses using si-control- and si-TAGLN2-transfected BC cell lines, however, there were no significant differences between the two groups (data not shown). Therefore, we expected that the promotion of apoptosis and cell cycle arrest by transfection of miR-1 and miR-133a were due to other mechanisms affected by these miRNAs, but it was not due to TAGLN2 down-regulation.

There was no significant relationship between the clinicopathological parameters and the expression levels of miR-1 and miR-133a, and none between the parameters and the TAGLN2 mRNA expression. This indicates that the down-regulation of these miRNAs and up-regulation of TAGLN2 might be early events in RCC progression. If not, since our cohort was not so large ($n = 40$) and included only ten samples of advanced cancer (more than pT2) and no samples of grade 3 cancer, studies on a larger number of samples with a balanced pathological background will have to be conducted to elucidate the precise correlation between them.

In conclusion, both miR-1 and miR-133a were significantly down-regulated in the RCC cell lines and the clinical specimens and functioned as a tumour suppressor. Our data indicate that up-regulation of the oncogenic TAGLN2 may be due to down-regulation of the tumour suppressive miR-1 and miR-133a in human RCC progression. This novel molecular network may play a critical role in RCC development and serve as a novel therapeutic strategy for patients with RCC.

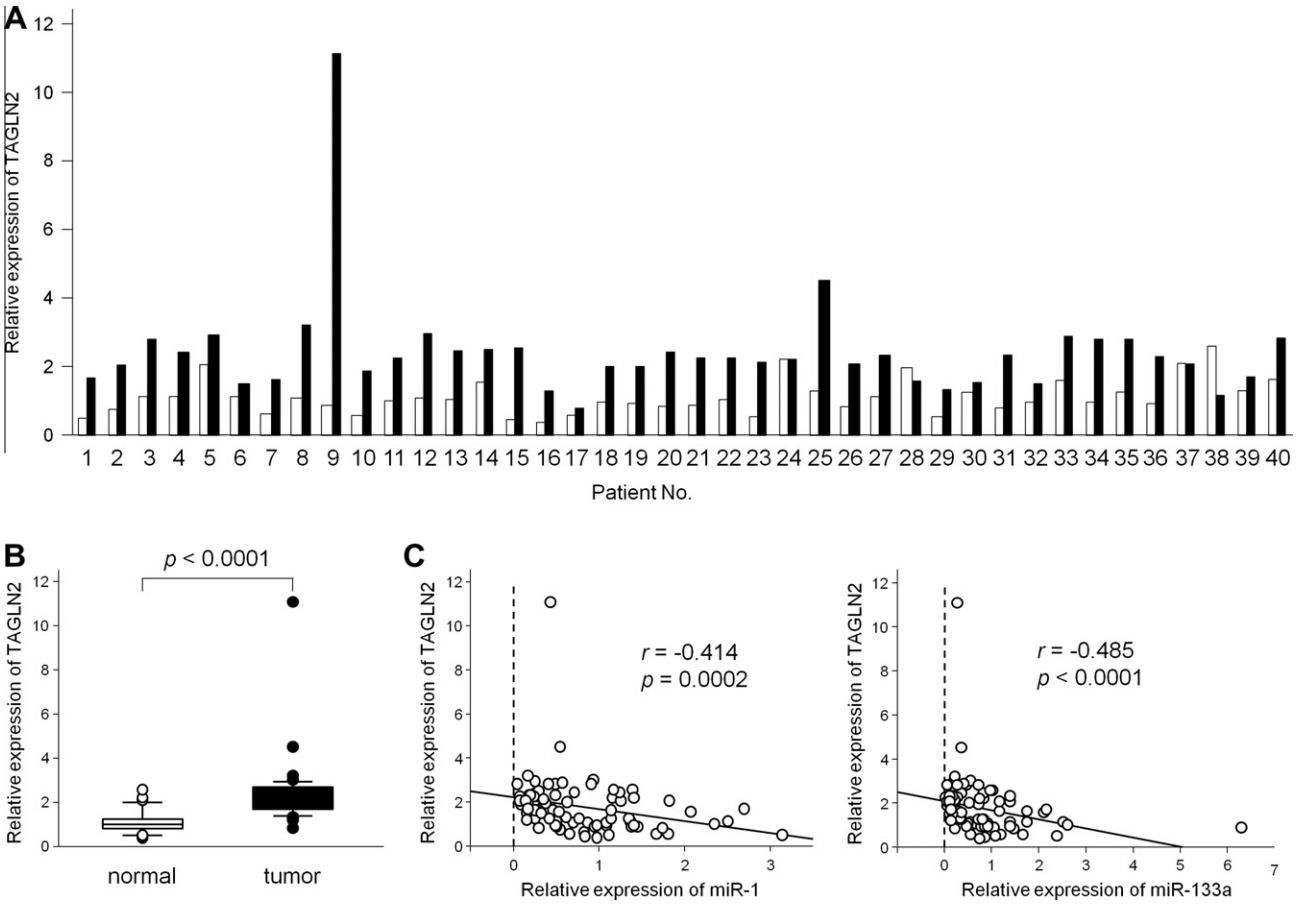

Fig. 6 – mRNA expression levels of TAGLN2 in RCC specimens. (A) Normalised relative mRNA expression levels of TAGLN2 are shown in the bar chart. White and black bars indicate the expression levels in normal and tumour tissues, respectively. (B) Relative mRNA expression level of TAGLN2 is expressed in the box plot. (C) Correlation between the relative expression levels of miR-1 and miR-133a (*x*-axis) and TAGLN2 (*y*-axis) (left and right, respectively). Levels are plotted as a scatter plot.

Role of the funding source

This research was partially supported by the Ministry of Education, Science, Sports and Culture Grants-in-Aid for Scientific Research (B and C), 20390427 and 20591861, 2008.

Conflict of interest statement

None declared.

Acknowledgements

We thank Ms. Mutsumi Miyazaki for her excellent laboratory assistance.

REFERENCES

1. Weng L, Wu X, Gao H, et al. MicroRNA profiling of clear cell renal cell carcinoma by whole-genome small RNA deep sequencing of paired frozen and formalin-fixed, paraffin-embedded tissue specimens. *J Pathol* 2010;**222**:41–51.
2. Fridman E, Dotan Z, Barshack I, et al. Accurate molecular classification of renal tumors using microRNA expression. *J Mol Diagn* 2010;**12**:687–96.
3. Aben KK, Luth TK, Janssen-Heijnen ML, et al. No improvement in renal cell carcinoma survival: a population-based study in The Netherlands. *Eur J Cancer* 2008;**44**:1701–9.
4. Bartel DP. MicroRNAs: genomics, biogenesis, mechanism, and function. *Cell* 2004;**116**:281–97.
5. Bader AG, Brown D, Winkler M. The promise of microRNA replacement therapy. *Cancer Res* 2010;**70**:7027–30.
6. Calin GA, Croce CM. MicroRNA signatures in human cancers. *Nat Rev Cancer* 2006;**6**:857–66.
7. Esquela-Kerscher A, Slack FJ. Oncomirs – microRNAs with a role in cancer. *Nat Rev Cancer* 2006;**6**:259–69.
8. Ichimi T, Enokida H, Okuno Y, et al. Identification of novel microRNA targets based on microRNA signatures in bladder cancer. *Int J Cancer* 2009;**125**:345–52.
9. Chiyomaru T, Enokida H, Tatarano S, et al. MiR-145 and miR-133a function as tumour suppressors and directly regulate FSCN1 expression in bladder cancer. *Br J Cancer* 2010;**102**:883–91.
10. Chiyomaru T, Enokida H, Kawakami K, et al. Functional role of LASP1 in cell viability and its regulation by microRNAs in bladder cancer. *Urol Oncol* (in press).

11. Uchida Y, Chiyomaru T, Enokida H, et al. MiR-133a induces apoptosis through direct regulation of GSTP1 in bladder cancer cell lines. *Urol Oncol* (in press).
12. Yoshino H, Chiyomaru T, Enokida H, et al. The tumour suppressive function of *miR-1* and *miR-133a* targeting TAGLN2 in bladder cancer. *Br J Cancer* 2011;**104**:808–18.
13. Song T, Xia W, Shao N, et al. Differential miRNA expression profiles in bladder urothelial carcinomas. *Asian Pac J Cancer Prev* 2010;**11**:905–11.
14. Liu R, Zhang C, Hu Z, et al. A five-microRNA signature identified from genome-wide serum microRNA expression profiling serves as a fingerprint for gastric cancer diagnosis. *Eur J Cancer* 2010;**47**:784–91.
15. Rao PK, Missiaglia E, Shields L, et al. Distinct roles for miR-1 and miR-133a in the proliferation and differentiation of rhabdomyosarcoma cells. *FASEB J* 2010;**24**:3427–37.
16. Yan D, Dong Xda E, Chen X, et al. MicroRNA-1/206 targets c-Met and inhibits rhabdomyosarcoma development. *J Biol Chem* 2009;**284**:29596–604.
17. Sarver AL, French AJ, Borralho PM, et al. Human colon cancer profiles show differential microRNA expression depending on mismatch repair status, are characteristic of undifferentiated proliferative states. *BMC Cancer* 2009;**9**:401.
18. Nasser MW, Datta J, Nuovo G, et al. Down-regulation of micro-RNA-1 (miR-1) in lung cancer. Suppression of tumorigenic property of lung cancer cells and their sensitization to doxorubicin-induced apoptosis by miR-1. *J Biol Chem* 2008;**283**:33394–405.
19. Ambs S, Prueitt RL, Yi M, et al. Genomic profiling of microRNA and messenger RNA reveals deregulated microRNA expression in prostate cancer. *Cancer Res* 2008;**68**:6162–70.
20. Datta J, Kutay H, Nasser MW, et al. Methylation mediated silencing of MicroRNA-1 gene and its role in hepatocellular carcinogenesis. *Cancer Res* 2008;**68**:5049–58.
21. Nohata N, Hanazawa T, Kikkawa N, et al. Caveolin-1 mediates tumor cell migration and invasion and its regulation by miR-133a in head and neck squamous cell carcinoma. *Int J Oncol* 2011;**38**:209–17.
22. Kano M, Seki N, Kikkawa N, et al. miR-145, miR-133a and miR-133b: Tumor suppressive miRNAs target FSCN1 in esophageal squamous cell carcinoma. *Int J Cancer* 2010;**127**:2804–14.
23. Wong TS, Liu XB, Chung-Wai Ho A, et al. Identification of pyruvate kinase type M2 as potential oncoprotein in squamous cell carcinoma of tongue through microRNA profiling. *Int J Cancer* 2008;**123**:251–7.
24. Sobin LH, Gospodarowicz MK, Wittekind C. TNM Classification of Malignant Tumours, 7th ed. International Union Against Cancer (UICC), Wiley-Liss; 2009. p. 255–257.
25. Nakada C, Matsuura K, Tsukamoto Y, et al. Genome-wide microRNA expression profiling in renal cell carcinoma: significant down-regulation of miR-141 and miR-200c. *J Pathol* 2008;**216**:418–27.
26. Zhang Y, Ye Y, Shen D, et al. Identification of transgelin-2 as a biomarker of colorectal cancer by laser capture microdissection and quantitative proteome analysis. *Cancer Sci* 2010;**101**:523–9.